Title

Development of an ATP-independent bioluminescent probe for detection of extracellular hydrogen peroxide.

Journal

Perkin 1, 20(31)

Authors

OSullivan, Justin

Heffern, Marie

Publication Date

2022-08-10

DOI

10.1039/d2ob00436d

Peer reviewed

HHS Public Access

Author manuscript

Org Biomol Chem. Author manuscript; available in PMC 2023 August 10.

Published in final edited form as:

Org Biomol Chem. ; 20(31): 6231–6238. doi:10.1039/d2ob00436d.

Development of an ATP-Independent Bioluminescent Probe for Detection of Extracellular Hydrogen Peroxide

Justin J. O'Sullivan[1], **Marie C. Heffern**[1]

[1]Department of Chemistry, University of California Davis, One Shields Drive, Davis, CA 95616, USA

Abstract

This work reports a new ATP-independent bioluminescent probe (bor-DTZ) for detecting hydrogen peroxide that is compatible with the Nanoluciferase enzyme. The probe is designed with an arylboronate ester protecting group appended to a diphenylterazine core via a self-immolative phenolate linker. Reaction with hydrogen peroxide reveals diphenylterazine, which can then react with Nanoluciferase to produce a detectable bioluminescent signal. Bor-DTZ shows a dose-dependent response to hydrogen peroxide and selectivity over other biologically relevant reactive oxygen species and can be applied to detect either intra- or extracellular species. We further demonstrate the ability of this platform to monitor fluxes in extracellular hydrogen peroxide in a breast cancer cell line in response to the anticancer treatments, cisplatin.

Introduction

Hydrogen peroxide (H_2O_2) is a key molecule in biological redox metabolism and stress.[1] On the one hand, H_2O_2 is a hallmark of oxidative stress[2] whereby its generation alongside other reactive oxygen species results in direct or indirect oxidation of various biomolecules such as lipids[3], DNA[4], RNA[5], and proteins[6]. On the other hand, endogenous levels of H_2O_2 have been shown to play important roles in cellular signaling in processes ranging from immune response to cell proliferation.[7,8,9,10,11] For example, neutrophils have been shown to utilize NADPH oxidase systems to generate millimolar quantities of H_2O_2 as a defense against foreign microbes.[12] H_2O_2 imbalances have been implicated in variety of disease pathologies such as cancer,[13,14] diabetes,[15,16] inflammation[17,18] and cardiovascular diseases[19,20]. Tools for monitoring H_2O_2 fluxes are vital for understanding the molecular mechanisms at play regarding both the physiological and pathological roles H_2O_2 plays in biological systems.

Small molecules[21,22,23,24,25] employing various reaction triggers such as sulfonic esters[22], diketones[26,27], and arylboronates[28] have been widely employed for fluorescence-based sensing of H_2O_2. In particular, the arylboronate reaction-based triggers have been

Author Contributions

J.J.O. and M.C.H. designed all experiments. J.J.O. performed all experiments and data collection. J.J.O. and M.C.H. analyzed the data. J.J.O. took the lead in writing the manuscript, and J.J.O. and M.C.H. wrote and edited the manuscript. M.C.H. conceived the study and was the major supervisor on overall direction of the study.

Conflict of Interest Statement

The authors report no conflicts of interest.

extensively adopted mainly owing to their high selectivity and sensitivity in addition to their fast reaction kinetics relative to other H_2O_2 reactive moieties.[29,30,31,32] Although fluorescence-based imaging probes have provided valuable insight into H_2O_2 dynamics, they are primarily applied to monitoring intracellular H_2O_2 dynamics, given that the larger volume and diffuse nature of the extracellular space and extracellular fluids can lead to signal dilution. Aside from fluorescence-based imaging probes researchers have also turned to the development of alternative modalities with improved sensitivity, such as such as electrochemical sensors, but many of these are not amenable to *in vivo* work.[33,34,35]

To fill this gap, bioluminescence has become an increasingly favorable candidate for molecular imaging platforms.[36] Bioluminescence results in the emission of photons via the enzymatic oxidation of a small molecule luciferin by its cognate luciferase enzyme. Imaging with this technique offers the benefits of high signal-to-noise ratio as well as the ability to endow cell and tissue specificity through the genetic encoding of the luciferase.[37] The phenomenon has been adapted for sensing molecular analytes of interest by chemical modification of the luciferin, termed "caging", which precludes interaction with its luciferase pair.[38,39] Upon chemo-selective reaction with the analyte the native luciferin is restored and subsequent oxidation by its luciferase results in the production of detectable photons. This strategy has been successfully employed for the detection of intracellular H_2O_2 using a firefly luciferin caged with an arylboronic acid.[40,41] While capable of detecting intracellular H_2O_2 and in the tissues of living mice, an inherent property of the firefly luciferin/luciferase system is its dependence on ATP, therefore limiting the probes' applicability to intracellular applications and regimes where ATP levels are not significantly perturbed. Development of probes for the extracellular space are of particular interest due to the transient nature of signaling biomolecules like H_2O_2. The ability to monitor extracellular H_2O_2 would provide valuable insight into both the physiological roles that this oxidative metabolite plays in extracellular signaling as well as a means to monitor oxidative stress in disease progression. Unlike the firefly luciferases, marine luciferases and their derivatives do not require ATP, making these platforms adaptable to extracellular applications.[42,43]

To this end, we report the design, synthesis, and evaluation of a new bioluminescent based probe for detecting H_2O_2 in the extracellular space using a marine luciferin/luciferase pair. We report a boronate ester caged diphenylterazine (bor-DTZ), a small molecule luciferin with an H_2O_2 reactive boronate ester and self-immolative linker attached to the carbonyl of the parent diphenylterazine (DTZ). Upon H_2O_2 induced oxidative hydrolysis and subsequent self-immolation, DTZ is generated which can then interact with the engineered marine luciferase, Nanoluciferase (Nluc)[44], to produce a detectable bioluminescent signal. We demonstrate the ability of bor-DTZ to selectively detect H_2O_2 over other biologically relevant ROS and show that it can detect exogenous and endogenous H_2O_2 in live cells. We further show the probes utility in monitoring changes to extracellular H_2O_2 in response to a clinically relevant cancer treatment in a human breast cancer cell model.

Results And Discussion

Synthesis and reactivity of bor-DTZ.

The recently engineered Nanoluciferase (Nluc) is a marine based luciferase derived from a deep sea shrimp which has gained attention due to its small size, high thermal stability, and highly intense luminescence in the presence of its engineered substrate, furimazine, relative to firefly luciferase.[44] We recently demonstrated that modifying imidazopyrazinone substrates at the imidazoyl carbonyl with a reactive group responsive to copper(II) could yield caged luciferins compatible with Nluc, with the synthetic imidazopyrazinone, diphenylterazine (DTZ), yielding optimal response among a series of caged imidazopyrazinone derivatives.[45] Thus, to design a bioluminescence agent for the Nluc system that could respond to hydrogen peroxide, we paired the well-studied arylboronate ester cage to diphenylterazine (DTZ) with a self-immolating phenolate linker (scheme 2). The arylboronate ester cage is expected to undergo selective oxidative hydroxylation by H_2O_2, which in turn triggers an electron cascade to reveal the parent DTZ for recognition by Nluc. We synthesized the native DTZ according to previously published methods[45, 46] and then performed a nucleophilic substitution with 4-bromomethylphenylboronic acid pinacol ester under basic conditions to afford bor-DTZ in 18% yield. We attributed the low yield due to a side product where the pinacol ester adds to the alkene at the C2 position as well as DTZ being inherently prone to oxidation. However, it is important to note that for subsequent biological assays bor-DTZ can be used in concentrations as low as 1 μM such that low milligram quantities of bor-DTZ can be used for hundreds of assays depending on sample size.

To evaluate the reactivity of bor-DTZ, its luminescence output was measured upon addition of analytes of interest in the presence of purified recombinant Nanoluciferase (rNluc) in aqueous buffer. Selectivity was assessed by comparing reactivity with H_2O_2 to a panel of reactive oxygen species as well as glutathione, a biologically relevant reducing agent. The normalized total photon flux was determined by calculating the area under the curve of the kinetic reading over 30 minutes and normalizing values from all ROS tested to that of bor-DTZ alone (Figure 1a). A representative kinetic curve for bor-DTZ in the presence of 100 μM H_2O_2 can be seen in the supplementary information (Figure S1). We observed that bor-DTZ exhibits exceptional selectivity towards H_2O_2 relative to the other ROS tested. We confirmed that the turn-on response was due to H_2O_2 by observing a loss in signal upon addition of catalase, an enzyme that rapidly degrades H_2O_2. The DTZ/Nluc system has been previously reported to have a λ_{max} of 500 nm.[46] The bor-DTZ/Nluc system similarly yielded a λ_{max} emission of 500 nm in the presence of H_2O_2 (Table S1), further confirming that the parent DTZ is released upon reaction with the analyte. Moreover, bor-DTZ demonstrated a dose-dependent response to the H_2O_2 from 50-250 μM (Figure 1b), which is within a biologically-relevant range in the context of the tumor microenvironment.[47,48,49] A 10-fold change in molar luminescence is observed from the lower limit of detection (10 μM H_2O_2) to the point of signal saturation (250 μM) (Table S1).

We next assessed whether the signal produced by bor-DTZ was affected by ATP. Previously reported bioluminescence probes for H_2O_2 rely on the firefly luciferase enzyme, which

utilizes ATP as a cofactor. The need for ATP limits the probe to mainly intracellular applications where ATP is abundant; additionally, various cellular processes can result in significant changes to ATP levels, making this cofactor a confounding variable for firefly luciferase-based sensors.

Detection of intracellular H_2O_2 by bor-DTZ.

Having established the selectivity and sensitivity of bor-DTZ towards H_2O_2 in buffer we next evaluated the H_2O_2 responsiveness in cells. We utilized a breast cancer cell line, MDA-MB-231, engineered to express Nluc intracellularly. To stimulate an increase in intracellular H_2O_2 we treated cells with 500 μM paraquat for 24 hours, which generates intracellular ROS through disruption of mitochondrial respiration.[50] We monitored light output in the presence of both bor-DTZ, and analogous experiments were performed using the parent DTZ. The data is presented as the ratio of the area under the curve of the 1 hour luminescence of bor-DTZ:DTZ in order to normalize for any changes in Nluc expression or cell proliferation due to paraquat treatment (Figure 2a). Representative kinetic curves for the luminescence of both bor-DTZ and DTZ are presented in the supplementary information (Figure S2). Indeed, bor-DTZ detected a significant ($p < 0.005$) increase in signal of paraquat-treated cells relative to untreated cells showing the biological utility of this probe in cell-based models. As this particular cell-line is expressing a form of Nluc without a secretion signaling domain the observed signal indicates that bor-DTZ is able to diffuse through the cell membrane. Additionally, the cells are washed with PBS prior to imaging in order to remove any extracellular hydrogen peroxide or Nluc that may be present. We also performed an experiment to assess the toxicity of bor-DTZ towards the cells using an MTS assay, and found that when Nluc MDA-MB-231 cells are incubated with bor-DTZ (10 μM) for 8 hours there is no significant effect on cell viability (Figure 2b), suggesting minimal to no toxicity.

Detection of extracellular H_2O_2 by bor-DTZ.

To determine the ability of bor-DTZ to detect changes in extracellular H_2O_2, we applied bor-DTZ in the media of MDA-MB-231 cells engineered to stably express and secrete Nanoluciferase (secNluc MDA-MB-23). Cells were plated and cultured in Optimem media for 24 hours, then media was removed and placed in a new well plate, H_2O_2 was spiked in and the samples were treated with bor-DTZ, then analyzed for light output over a 20-minute period. As the cells secrete Nluc, no addition of rNluc was required for these experiments. Furthermore, media was removed from cells and the assay was done in the absence of cells to prevent any signal occurring from intracellular activation. We observed slight increases in light output in the 0-10 μM range followed by large increases from 50-250 μM (Figure 3a). This range is in line with physiologically-relevant levels of tumor microenvironments wherein H_2O_2 concentrations can reach as high as 50-100 μM.[47,48,49]

To determine if bor-DTZ could detect endogenous levels of H_2O_2 in the media, the bioluminescent response of the media was measured in the absence or presence of catalase without addition of exogenous H_2O_2 (Figure 2b). We observe a drastic decrease in light output in cell media that had been spiked with catalase suggesting bor-DTZ could detect basal levels of H_2O_2 in the media. Notably, catalase has little to no effect on the native DTZ/Nluc system (Figure S3).

As oxidative stress and ROS production is a hallmark of breast cancer,[51] we applied bor-DTZ to assess how extracellular H_2O_2 levels are perturbed in the presence of cisplatin, a well-studied anti-cancer agent.[52] The secNluc MDA-MB-231 cells were plated and treated with cisplatin for 16 hours before removing the media from the cells and monitoring luminescence in the presence of bor-DTZ or the parent DTZ for 20 minutes. The ratio of the area under the curve for bor-DTZ:DTZ was calculated in order to account for any effects that the treatments had on secNluc expression or cell proliferation (Figure 3c). We observe that cisplatin treatment induces a decrease in light output relative to the control. Interestingly, our previous report on a copper(II) responsive DTZ showed that cisplatin also decreases extracellular levels of copper(II). These findings provide a basis and tool for further investigations into the interplay between trafficking of H_2O_2 and copper in both physiological and pathological states. The above study also demonstrates the high-throughput and accessible nature that the bor-DTZ probe offers through use of a 96-well plate and luminometer or plate reader. This lays the foundation for a unique new tool for future high-throughput studies investigating the effect of external stimuli on H_2O_2 dynamics.

Experimental Methods

General Methods.

Reactions using moisture- or air-sensitive reagents were carried out in dried glassware under an inert N_2 atmosphere. DTZ (**4)** was synthesized according to previously published methods.[45,46] Dry solvents were all purchased from Sigma-Aldrich and used immediately. All commercially purchased chemicals were used as received without further purification. 2-aminopyrazine was purchased from Oakwood Products. All other chemicals were purchased from Sigma-Aldrich unless otherwise noted. Silica Gel 60 F254 (precoated sheets, 200 μm thickness, MilliporeSigma) were used for analytical thin layer chromatography. Silica gel sorbent (230-400 mesh, grade 60, ThermoFisher) or aluminum oxide (neutral, Brockmann I, 50-200 μm, grade 60, Sigma-Aldrich) were used for column chromatography. ^{1}H and ^{13}C NMR spectra were collected at room temperature in DMSO-d6 (Sigma-Aldrich) on a 600 MHz Varian NMR spectrometer. All chemical shifts are reported as δ parts per million relative to the residual solvent peak at 2.50 (DMSO-d6) for 1H and 39.52 (DMSO-d6) for 13C. Multiplicities are reported as s (singlet), d (doublet), t (triplet), q (quartet), p (pentet), h (hextet), m (multiplet), dt (doublet of triplets), or br (broad). Heated electrospray ionization mass spectral analyses were performed using an ThermoQ Exactive HF (High field Orbitrap) at the UC Davis Campus Mass Spectrometry Facilities.

Synthesis of bor-DTZ.

Diphenylterazine, **4**, (14 mg, 0.037 mmol, 1 equiv.), 4-bromomethylphenylboronic acid pinacol ester (11 mg, 0.037 mmol, 1 equiv.), Cs_2CO_3 (5 mg, 0.015 mmol, 0.4 equiv.), and KI (7 mg, 0.041 mmol, 1.1 equiv.) were added to a flame-dried round-bottom flask that was then purged with N_2. The reagents were then dissolved in anhydrous acetonitrile (1 mL) and the reaction was allowed to stir overnight. The reaction mixture was subsequently quenched in 10 mL of water and extracted in DCM (3 x 5 mL). The combined DCM extract was then washed with brine, dried over Na_2SO_4, and concentrated under reduced

pressure. The crude product was then purified by reverse-phase HPLC (isochratic, 80/20 MeCN:H_2O over 2 hours on a T3 Atlantis column (Waters)) and dried under reduced pressure to obtain **bor-DTZ** (4 mg, 18% yield) as a yellow-brown solid. ^{1}H NMR (600 MHz, DMSO-d6) δ 8.83-8.85 (d, 2H), 8.44 (s, 1H), 8.09-8.11 (d, 2H), 7.68-7.70 (d, 2H), 7.50-7.60 (m, 5H), 7.46-7.47 (d, 2H), 7.41-7.43 (t, 1H), 7.27 (m, 4H), 7.18 (m, 1H), 5.25 (s, 2H), 4.07 (s, 2H), 1.27 (s, 12H). ^{13}C NMR (151 MHz, DMSO-d6) δ 146.08, 139.64, 139.59, 137.25, 137.11, 136.84, 136.19, 135.09, 134.15, 131.55, 130.77, 129.75, 129.17, 129.13, 129.03, 128.88, 128.86, 128.82, 128.74, 126.62, 126.48, 110.99, 84.18, 77.02, 32.95, 25.11. High-resolution mass spectrometry (HRMS) (m/z): $[M+H]^+$ calculated for : $C_{38}H_{37}BN_3O_3$, 594.2927; found, 594.2915.

In Vitro Luminescence Assays.

Milli-Q water (18.2 MΩ) was used to prepare all aqueous solutions. Reactive oxygen species solutions were prepared to 10 mM in water. Hydrogen peroxide (H_2O_2), *tert*-butyl hydroperoxide (TBHP), and hypochlorite (OCl^-) stock solutions were prepared from 30%, 70%, and 2-3% aqueous solutions, respectively. Hydroxyl radical (*OH) and *tert*-butoxy radical (*OtBu) were generated in situ by reaction with excess Fe(II). Nitric oxide (NO*) was generated using PROLI NONOate (Cayman Chemical). Superoxide (O_2^-) was delivered from a stock solution of potassium superoxide (KO_2) in DMSO. A 100 μM solution of bor-DTZ was prepared by dissolving bor-DTZ in pure ethanol. A 0.4 μg/mL solution of rNluc was prepared by adding 1 μL of 0.4 mg/mL stock solution (Promega, Nano-Glo Assay Kit) into 999 μL of DPBS at pH 7.4. 100 μL of rNluc solution was added to the wells of a white, opaque, flat-bottom 96-well plate followed by 1 μL of ROS 10 mM stock solution or 1 μL of a 1 M GSH stock solution.. Finally, bor-DTZ (1 μL) was added to all the wells using a multichannel pipette and mixed well. The bioluminescent signal was immediately measured using a Molecular Devices SpectraMax i3x plate reader at 37 °C for 1 hour. For dose-dependence studies 100x stock solutions of H_2O_2 were prepared in Millipore water from a 30% (w/w/) aqueous solution and 1 μL of these stock solutions were added to 100 uL of rNluc solution in wells of a 96-well white plate. Bor-DTZ (1 μL of a 100 μM solution) was added via a multichannel pipette and the luminescence was immediately measured. For ATP studies a 10 mM solution of ATP was prepared in DPBS pH 7.4 by adding 100 μL of a 100 mM stock (ThermoScientific) into 900 μL of DPBS. To this was added 1 μL of 0.4 mg/mL rNluc (Promega) to get a final volume of 0.4 μg/mL rNluc. The control rNluc solution was prepared to 0.4 μg/mL as described previously and 100 μL aliquots of control and ATP containing solutions were plated in 96-well white plate. Bor-DTZ (1 μL of a 100 μM solution) was added to the wells and the luminescence was measured immediately. When reporting area under the curve, these values were calculated using GraphPad Prism software.

Cell Culture.

MDA-MB-231 cells stably expressing secreted or intracellular Nanoluciferase (secNluc MDA-MB-231 or Nluc MDA-MB-231 respectively) were a kind gift from Drs. Gary and Kathy Luker (University of Michigan). Cells were maintained in Dulbecco's modified medium (DMEM, 4.5 g/L glucose) supplemented with 10% fetal bovine serum (FBS)

(Gibco) 1x penicillin-streptomycin (Corning), 2 mM L-glutamine (Gibco), 1 mM sodium pyruvate (Gibco) at 37 °C and 5% CO_2.

Detecting H_2O_2 intracellularly in Nluc MDA-MB-231 Cells.

Cells were plated at 10,000 cells per well in a 96-well white, opaque, flat bottom plate. Twenty-four hours later media was replaced with fresh media and paraquat was added from a freshly prepared stock solution to a final concentration of 500 μM. Cells were then incubated for 24 hours and then the media was removed and washed with warm DPBS before adding 100 μL of fresh DPBS to wells. Bor-DTZ (1 μL of a 1 mM solution) was added to wells and luminescence was measured immediately over one hour.

MTS Assay of Bor-DTZ treated Nluc MDA-MB-231 Cells.

Cells were plated at 10,000 cells per well in a 96-well black, clear bottom plate. Twenty-four hours later the media was replaced with fresh media (containing no FBS) and Bor-DTZ (stock solution in ethanol) was added to wells at a final concentration of 10 μM and the plate was incubated for 8 hours in a 37°C incubator and 5% CO_2. Following incubation MTS (CellTiter 96, Promega) was added to wells according to the manufacturers protocol. The plate was incubated for one hour at 37 °C before measuring the absorbance at 490 nm on a Molecular Devices SpectraMax i3x.

Detecting H_2O_2 in Media of secNluc MDA-MB-231 Cells.

Cells were plated at 10,000 cells per well in a 96-well black clear bottom plate. Twenty-four hours later the media was removed from the wells and added to a fresh 96-well white, opaque, flat bottom plate. Catalase (Sigma Aldrich) was added to wells in triplicate to a final concentration of 1 x 104 U/L from a stock solution. Following this bor-DTZ (1 μL of a 100 μM solution) was added to wells and luminescence was measured immediately. For dose-response experiments 100X solutions of H_2O_2 were prepared in water and 1 μL of this was added to secNluc MDA-MB-231 cells 24 hours after plating as previously described. Bor-DTZ (1 μL of a 100 μM solution) was added to wells and luminescence was measured immediately.

Monitoring secNluc MDA-MB-231 response to cisplatin.

Cells were plated at 10,000 cells per well in a 96-well, white, opaque flat-bottom plate. Eight hours later, the media was removed, and the cells were washed with pre-warmed (37 °C) DPBS and 100 μL of OptiMem (Gibco) was added to each well. A 3 mM solution of cis-platin was prepared in water. 1 μL of this was added to the wells for a final concentration of 30 μM cisplatin. At the 16-hour time point solutions of 100 μM bor-DTZ and 100 μM DTZ (in ethanol) were prepared and 1 μL was added per well per treatment (n=3). Luminescence was immediately recorded as previously described. The area under the curve was calculated using GraphPad Prism software and the ratio of the A.U.C. from bor-DTZ to DTZ was calculated.

Conclusions

We have demonstrated the design, synthesis, and evaluation of a new bioluminescent probe, bor-DTZ, for monitoring H_2O_2 in vitro in an ATP-independent manner. Bor-DTZ shows a high level of selectivity towards H_2O_2 over other biologically relevant reactive oxygen species and shows sensitivity down to the low-mid μM range. The probe can detect H_2O_2 in either intracellular or extracellular environments based on where the Nluc enzyme is expressed. We also demonstrate that bor-DTZ can be applied to a 96 well-plate for cell-based assays for high-throughput analysis of H_2O_2 dynamics in a cancer cell line.

Bioluminescence-based sensing of H_2O_2 offers the advantages of in vivo compatibility as well as high sensitivity due to near-zero background and signal output that does not require an excitation light source. Among the caged bioluminescence agents that have been reported, bor-DTZ is one of the first diphenylterazine-based imaging probes to be paired with the bright, thermostable Nluc. The ATP-independent nature of Nluc allows bor-DTZ to be used in both intracellular and extracellular applications broadening the scope of currently available tools for H_2O_2. Paired with Nluc and emerging analogs for deep-tissue imaging, bor-DTZ has broad potential for investigating oxidative biology in both cell-based and live-animal studies.

Supplementary Material

Refer to Web version on PubMed Central for supplementary material.

Acknowledgements

This work was supported by the National Institute of Health (NIH MIRA 5R35GM133684-02), the National Science Foundation (NSF CAREER 2048265). We also thank the Hartwell Foundation for their generous support for M.C.H. as a Hartwell Individual Biomedical Investigator, as well as the UC Davis CAMPOS Program and the University of California's Presidential Postdoctoral Fellowship Program for their support of M.C.H. as a CAMPOS Faculty Fellow and former UC President's Postdoctoral Fellow, respectively. This work was also supported in part by gift funds from the UC Davis Comprehensive Cancer Center. We thank Dr's Gary and Kathy Luker (University of Michigan) for gifting MDA-MB-231 cell lines stably expressing secreted Nanoluciferase. We thank Samuel Janisse for running HRMS.

Notes and References

(1). Brandes RP; Weissmann N; Schroöder K Free Radical Biology and Medicine Nox Family NADPH Oxidases : Molecular Mechanisms of Activation. Free Radio. Biol. Med 2014, 76, 208–226.

(2). Rojkind M; Domínguez-rosales J; Nieto N; Greenwel P Role of Hydrogen Peroxide and Oxidative Stress. Cell. Mol. Life Sci 2002, 59, 1872–1891. [PubMed: 12530519]

(3). Siddique YH; Ara G; Afzal M Estimation of Lipid Peroxidation Induced by Hydrogen Peroxide in Cultured Human Lymphocytes. Dose-Response 2012, 10, 1–10. [PubMed: 22423225]

(4). Valverde M; Lozano-salgado J; Fortini P; Rodriguez-sastre MA; Rojas E; Dogliotti E Hydrogen Peroxide-Induced DNA Damage and Repair through the Differentiation of Human Adipose-Derived Mesenchymal Stem Cells. Stem Cells Int. 2018, 2018.

(5). Liu M; Gong X; Alluri RK; Wu J; Sablo T; Li Z Characterization of RNA Damage under Oxidative Stress in Escherichia Coli Min. 2012, 393 (3), 123–132.

(6). Zhu H; Tamura T; Fujisawa A; Nishikawa Y; Cheng R; Takato M; Hamachi I Imaging and Profiling of Proteins under Oxidative Conditions in Cells and Tissues by Hydrogen-Peroxide-Responsive Labeling. J. Clin. Exp. Hepatol 2020, 142, 15711–15721.

(7). Stone JR; Yang S Hydrogen Peroxide: A Signaling Messenger. Antioxid. Redox Signal 2006, 8 (3), 243–270. [PubMed: 16677071]

(8). Lennicke C; Cocheme HM Review Redox Metabolism: ROS as Specific Molecular Regulators of Cell Signaling and Function. Mol. Cell 2021, 81, 3691–3707. [PubMed: 34547234]

(9). Autréaux BD; Toledano MB REVIEWS ROS as Signalling Molecules: Mechanisms That Generate Specificity in ROS Homeostasis. Nat. Rev. Mol. Cell Biol 2007, 8, 813–824. [PubMed: 17848967]

(10). Cotter TG; Gough DR Hydrogen Peroxide: A Jekyll and Hyde Signalling Molecule. Cell Death Dis. 2011, 2, 1–8.

(11). Antunes F; Brito PM Redox Biology Quantitative Biology of Hydrogen Peroxide Signaling. Redox Biol. 2017, 13, 1–7. [PubMed: 28528123]

(12). Rhee SG H2O2, a Necessary Evil for Cell Signaling. Science. 2006, 312 (5782), 1882–1884. [PubMed: 16809515]

(13). Gupte A; Mumper RJ Elevated Copper and Oxidative Stress in Cancer Cells as a Target for Cancer Treatment. Cancer Treat. Rev 2009, 35 (1), 32–46. [PubMed: 18774652]

(14). Finkel T; Serrano M; Blasco MA The Common Biology of Cancer and Ageing. Nat. Rev 2007, 448, 767–774.

(15). Wang W; Jiang W; Mao G; Tan M; Fei J; Li Y; Li C Monitoring the Fluctuation of Hydrogen Peroxide in Diabetes and Its Complications with a Novel Near-Infrared Fluorescent Probe. Anal. Chem 2021, 93, 3301–3307. [PubMed: 33535747]

(16). Houstis N; Rosen ED; Lander ES Reactive Oxygen Species Have a Causal Role in Multiple Forms of Insulin Resistance. Nature 2006, 440, 944–948. [PubMed: 16612386]

(17). Wittmann C; Chockley P; Singh SK; Pase L; Lieschke GJ; Grabher C Hydrogen Peroxide in Inflammation : Messenger , Guide , and Assassin. Adv. Hematol 2012, 2012, 1–6.

(18). Mittal M; Siddiqui MR; Tran K; Reddy SP; Malik AB Reactive Oxygen Species in Inflammation and Tissue Injury. Antioxid. Redox Signal 2014, 20 (7), 1126–1167. [PubMed: 23991888]

(19). Steinhorn B; Michel T Chemogenetic Generation of Hydrogen Peroxide in the Heart Induces Severe Cardiac Dysfunction. Nat. Commun 2018, 9, 4044. [PubMed: 30279532]

(20). Horwitz D; Sherman NA; Horwitz D Hydrogen Peroxide Cytotoxicity in Cultured Cardiac Myocytes Is Iron Dependent. Hear. Circ. Physiol 1994, 226 (1), 121–127.

(21). Lampard EV; Sedgwick AC; Sun X; Filer KL; Hewins SC Boronate-Based Fluorescence Probes for the Detection of Hydrogen Peroxide. ChemistryOpen 2018, 262–265. [PubMed: 29531890]

(22). Maeda H; Fukuyasu Y; Yoshida S; Fukuda M; Saeki K; Matsuno H; Yamauchi Y; Yoshida K; Hirata K; Miyamoto K Fluorescent Probes for Hydrogen Peroxide Based on a Non-Oxidative Mechanism. Angew. Chemie 2004, 43, 2389–2391.

(23). Dickinson BC; Huynh C; Chang CJ A Palette of Fluorescent Probes with Varying Emission Colors for Imaging Hydrogen Peroxide Signaling in Living Cells. J. Am. Chem. Soc 2010, 23, 5906–5915.

(24). Chang MCY; Pralle A; Isacoff EY; Chang CJ A Selective , Cell-Permeable Optical Probe for Hydrogen Peroxide in Living Cells. J. Am. Chem. Soc 2004, 2, 15392–15393.

(25). Soh N Recent Advances in Fluorescent Probes for the Detection of Reactive Oxygen Species. Anal. Bioanal. Chem 2006, 386, 532–543. [PubMed: 16609844]

(26). Xie X; Wu T; Li Y; Li M; Tan Q; Wang X; Tang B Rational Design of an α - Ketoamide-Based Near-Infrared Fluorescent Probe Speci Fi c for Hydrogen Peroxide in Living Systems. Anal. Chem 2016, 88, 8019–8025. [PubMed: 27442152]

(27). Abo M; Urano Y; Hanaoka K; Terai T; Komatsu T; Nagano T Development of a Highly Sensitive Fluorescence Probe for Hydrogen Peroxide. J. Am. Chem. Soc 2011, 133, 10629–10637. [PubMed: 21692459]

(28). Carroll V; Michel BW; Blecha J; Vanbrocklin H; Keshari K; Wilson D; Chang CJ A Boronate-Caged [18 F]FLT Probe for Hydrogen Peroxide Detection Using Positron Emission Tomography. J. Am. Chem. Soc 2014, 136 (42), 14742–14745. [PubMed: 25310369]

(29). Miller EW; Albers AE; Pralle A; Isacoff EY; Chang CJ Boronate-Based Fluorescent Probes for Imaging Cellular Hydrogen Peroxide. J. Am. Chem. Soc 2005, 127 (47), 16652–16659. [PubMed: 16305254]

(30). Lippert AR; Bittner GCVANDE; Chang CJ Boronate Oxidation as a Bioorthogonal Reaction Approach for Studying the Chemistry of Hydrogen Peroxide in Living Systems. Acc. Chem. Res 2011, 44 (9), 793–804. [PubMed: 21834525]

(31). Purdey MS; Mclennan HJ; Sutton-mcdowall ML; Drumm DW; Zhang X; Capon PK; Heng S; Thompson JG; Abell AD Sensors and Actuators B : Chemical Biological Hydrogen Peroxide Detection with Aryl Boronate and Benzil BODIPY-Based Fluorescent Probes. Sensors Actuators B. Chem 2018, 262, 750–757.

(32). Chen Y; Shi X; Lu Z; Wang X; Wang Z A Fluorescent Probe for Hydrogen Peroxide in Vivo Based on the Modulation of Intramolecular Charge Transfer. Anal. Chem 2017, 89, 5278–5284. [PubMed: 28415838]

(33). Hosogi S; Marunaka Y; Ashihara E; Yamada T Plasma Membrane Anchored Nanosensor for Quantifying Endogenous Production of H2O2 in Living Cells. Biosens. Bioelectron 2021, 179, 113077. [PubMed: 33607416]

(34). Zhang T; Gu Y; Li C; Yan X; Lu N; Liu H; Zhang Z; Zhang H Fabrication of Novel Electrochemical Biosensor Based on Graphene Nanohybrid to Detect H 2 O 2 Released from Living Cells with Ultrahigh Performance. Appl. Mater. Interfaces 2017, 9, 37991–37999.

(35). Shen R; Liu P; Zhang Y; Yu Z; Chen X; Zhou L; Nie B; Chen J; Liu J Sensitive Detection of Single-Cell Secreted H 2 O 2 by Integrating a Micro Fl Uidic Droplet Sensor and Au Nanoclusters †. Anal. Chem 2018, 90, 4478–4484. [PubMed: 29510622]

(36). Rathbun CM; Prescher JA Bioluminescent Probes for Imaging Biology beyond the Culture Dish. Biochemistry 2017, 56, 5178–5184. [PubMed: 28745860]

(37). Mezzanotte L; van 't Root M; Karatas H; Goun EA; Löwik CWGM In Vivo Molecular Bioluminescence Imaging: New Tools and Applications. Trends Biotechnol. 2017, 35 (7), 640–652. [PubMed: 28501458]

(38). Li J; Chen L; Du L; Li M Cage the Firefly Luciferin! - A Strategy for Developing Bioluminescent Probes. Chem. Soc. Rev 2013, 42 (2), 662–676. [PubMed: 23099531]

(39). Yang X; Li Z; Jiang T; Du L; Li M A Coelenterazine-Type Bioluminescent Probe for Nitroreductase Imaging. Org. Biomol. Chem 2018, 16, 146–151.

(40). Bittner G. C. Van De; Dubikovskaya EA; Bertozzi CR; Chang CJ In Vivo Imaging of Hydrogen Peroxide Production in a Murine Tumor Model with a Chemoselective Bioluminescent Reporter. PNAS 2010, 21316–21321. [PubMed: 21115844]

(41). Van de Bittner GC; Bertozzi CR; Chang CJ Strategy for Dual-Analyte Luciferin Imaging: In Vivo Bioluminescence Detection of Hydrogen Peroxide and Caspase Activity in a Murine Model of Acute In Fl Ammation. J. Am. Chem. Soc 2013, 135, 1783–1795. [PubMed: 23347279]

(42). Yeh H; Xiong Y; Wu T; Chen M; Ji A; Li X; Ai H ATP-Independent Bioluminescent Reporter Variants To Improve in Vivo Imaging. ACS Chem. Biol 2019, 14, 959–965. [PubMed: 30969754]

(43). Markova SV; Larionova MD; Vysotski ES Shining Light on the Secreted Luciferases of Marine Copepods : Current Knowledge and Applications. Photochem. Photobiol 2019, 95 (2), 705–721. [PubMed: 30585639]

(44). Hall MP; Unch J; Binkowski BF; Valley MP; Butler BL; Wood MG; Otto P; Zimmerman K; Vidugiris G; MacHleidt T; et al. Engineered Luciferase Reporter from a Deep Sea Shrimp Utilizing a Novel Imidazopyrazinone Substrate. ACS Chem. Biol 2012, 7 (11), 1848–1857. [PubMed: 22894855]

(45). O'Sullivan JJ; Medici V; Heffern MC A Caged Imidazopyrazinone for Selective Bioluminescence Detection of Labile Extracellular Copper(II). Chem. Sci, 2022, 13, 4352. [PubMed: 35509459]

(46). Yeh H; Karmach O; Ji A; Carter D; Martins-green MM; Ai H Red-Shifted Luciferase – Luciferin Pairs for Enhanced Bioluminescence Imaging. Nat. Methods 2017, 14 (10), 971–978. [PubMed: 28869756]

(47). Chen Q; Liang C; Sun X; Chen J; Yang Z; Zhao H; Feng L; Liu Z H2O2-Responsive Liposomal Nanoprobe for Photoacoustic Inflammation Imaging and Tumor Theranostics via in Vivo Chromogenic Assay. PNAS 2017 114 (21), 5343–5348. [PubMed: 28484000]

(48). Chen Q; Feng L; Liu J; Zhu W; Dong Z; Wu Y Intelligent Albumin −MnO2 Nanoparticles as PH-/H2O2-Responsive Dissociable Nanocarriers to Modulate Tumor Hypoxia for Effective Combination Therapy. Advanced Mater. 2016, 28, 7129–7136.

(49). Szatrowski TP; Nathan CF Production of Large Amounts of Hydrogen Peroxide by Human Tumor Cells. Cancer Res. 1991, 51, 794–798. [PubMed: 1846317]

(50). Castello PR; Drechsel DA; Patel M Mitochondria Are a Major Source of Paraquat-Induced Reactive Oxygen Species Production in the Brain *. J. Biol. Chem 2007, 282 (19), 14186–14193. [PubMed: 17389593]

(51). Brown NS; Bicknell R Hypoxia and Oxidative Stress in Breast Cancer Oxidative Stress: Its Effects on the Growth , Metastatic Potential and Response to Therapy of Breast Cancer. Breast Cancer Res. 2001, 3 (5), 323–327. [PubMed: 11597322]

(52). Polishchuk RS Activity and Trafficking of Copper-Transporting ATPases in Tumor Development and Defense against Platinum-Based Drugs. Cells 2019, 8, 1080.

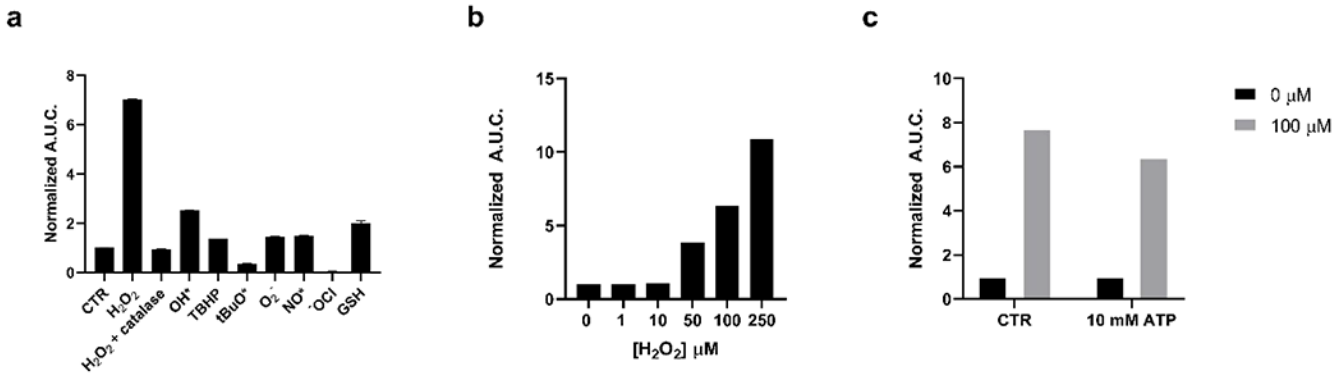

Figure 1.

Reactivity of bor-DTZ (1µM) reported as calculated area under the curve of luminescence output over 20 minutes in the presence of analytes and rNluc (0.4 µg/mL), normalized to bor-DTZ in the absence of analytes; all solutions in DPBS, pH 7.4, 37°C, emission range: 300-850 mn. (a) Reactivity of bor-DTZ in the presence of various biologically relevant ROS (100 µM) and glutathione (GSH, 10 mM). Error bars denote n=3, SEM. (b) Light output of bor-DTZ in the presence of various concentrations of H_2O_2 (0-250 µM) and rNluc (0.4 µg/mL). (c) Responsiveness of bor-DTZ to H_2O_2 (100 µM) in the presence of ATP (10 mM). Data points are normalized to the control without H_2O_2 added.

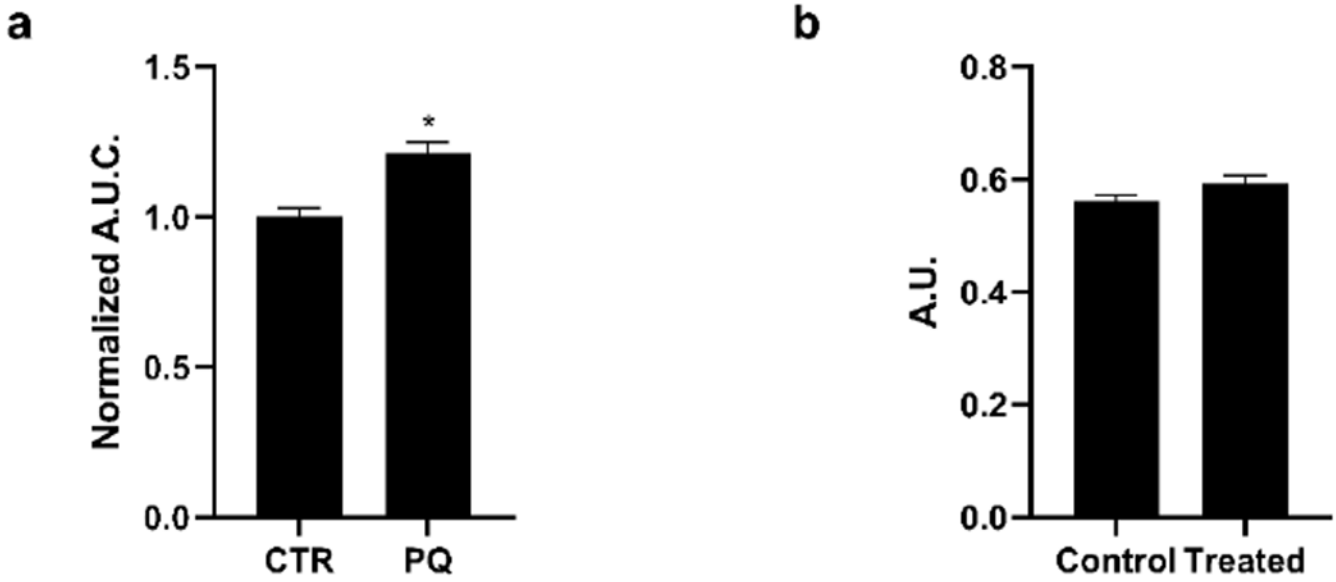

Figure 2.

(a) Calculated ratio of the area under the curve over 1 hour of bor-DTZ:DTZ (10 μM for both) luminescence from MDA-MB-231 cells expressing Nluc in the absence (control, CTR) or presence of 500 μM paraquat (PQ) for 24 hour's. Error bars denote n=3, SEM. Statistical significance was assessed by calculating *p*-values using unpaired t-test, * $p <$ 0.005. Measurements performed in DPBS, pH 7.4, 37°C, emission range: 300-850 mn. (b) Average absorbance at 490 mn of Nluc MDA-MB-231 cells after an 8-hour incubation with bor-DTZ (10 μM) followed by the addition of MTS for one hour. Error bars denote n=6.

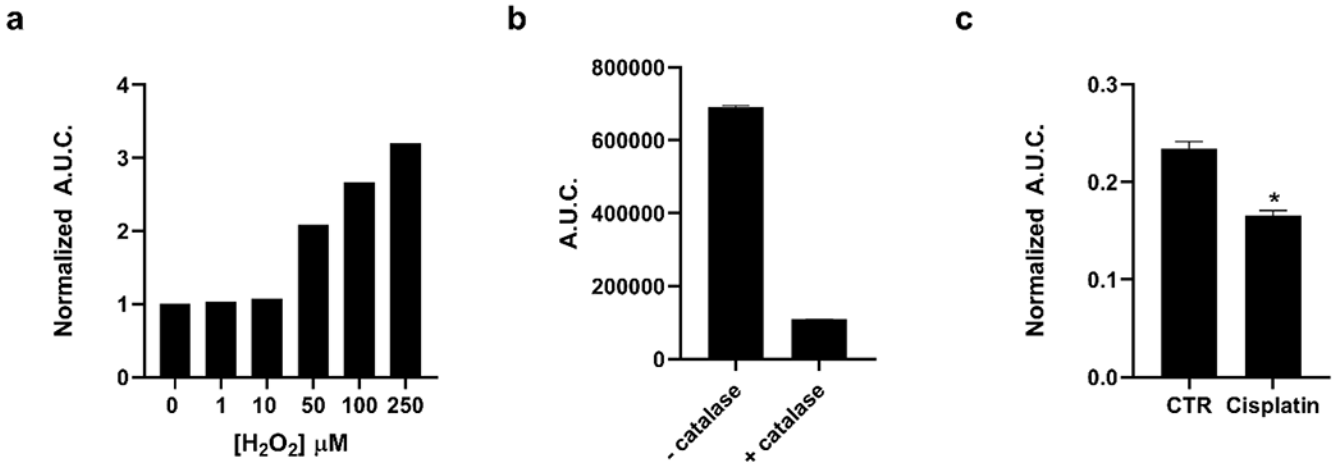

Figure 3.

(a) Dose-dependent light output as monitored by calculated area under the curve for luminescence over 20 minutes of bor-DTZ (1 μM) in the presence of various concentrations of H_2O_2 (0-250 μM) in cell media removed from secNluc MDA-MB-231 cells. Data points are normalized to the control without H_2O_2 added. (b) Calculated area under the curve of luminescence over 20 minutes of cell media from secNluc MDA-MB-231 cells in the presence or absence of catalase (1 x 10^4U/L) with 1 μM bor-DTZ. Error bars denotes SEM, n=3. (c) Calculated ratio of the area under the curve over 20 minutes of bor-DTZ:DTZ luminescence from secNluc MDA-MB-231 cells treated with cisplatin (30 μM). Error bars denote SEM, n=3. Statistical significance was assessed by calculating *p*-values using unpaired t-test,* $p < 0.05$. Measurements performed in Optimem, pH 7.4, 37°C, emission range: 300-850 mn.

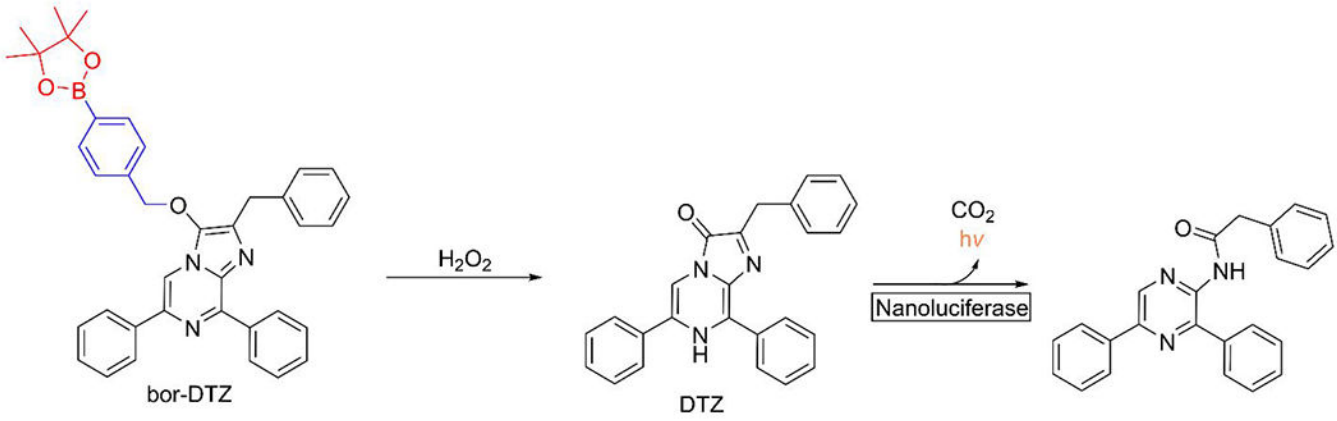

Scheme 1. Design of bor-DTZ for H_2O_2-responsive Bioluminescence[a]

[a] Red: H_2O_2-responsive cage, blue: self-immolative linker, black: diphenylterazine (DTZ) core.

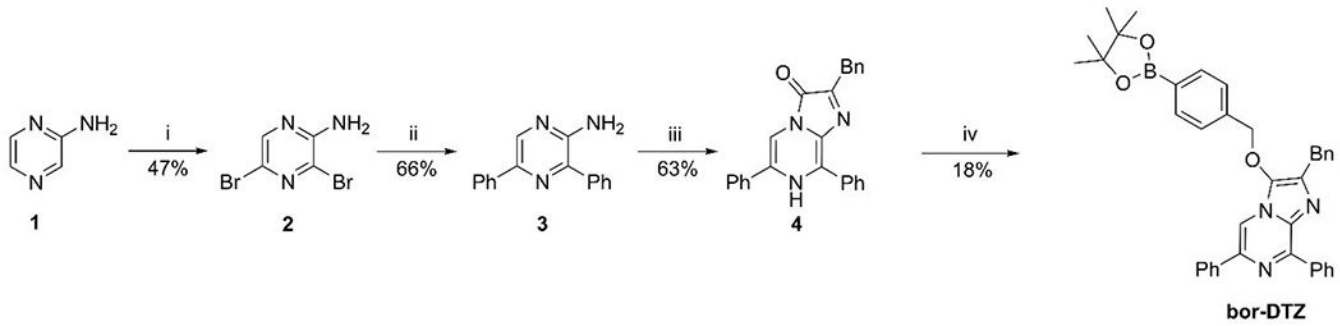

Scheme 2. Synthesis of bor-DTZ.

[a] **Reagents and conditions:** (i) NBS, $CHCl_3$, 3 h; (ii) Phenylboronic acid, $Pd(PPh_3)_4$, K_2CO_3, 1,4-dioxane, H_2O, 80 °C, 12 h; (iii) 1,1-diethoxy-3-phenylpropan-2-one, EtOH, H_2O, cat. HCl, 80 °C, 12 h; (iv) 4-Bromomethylphenylboronic acid pinacol ester, Cs_2CO_3, KI, MeCN, 12 h.